Report on a problem studied at the UK Mathematics-in-Medicine Study Group Strathclyde 2004
< http://www.maths-in-medicine.org/uk/2004/arterial-stents/ >

Arterial stents: modelling drug release and restenosis

J.E.F. Green[1], G.W. Jones[2], L.R. Band[1] and A. Grief[1]

[1]Centre for Mathematical Medicine, School of Mathematical Sciences,
University of Nottingham, Nottingham, NG7 2RD, UK.
[2] OCIAM, Mathematical Institute, University of Oxford, Oxford, UK.

1 Biological background

An arterial stent is a contemporary medical device used to prevent ischemia (inadequate blood flow) caused by the growth of an atherosclerotic plaque inside an artery wall.

Artery walls have three layers. The inner layer is the intima; this contains the endothelium, a layer of cells directly next to the blood which play an important role in controlling vascular tone, regulating transport into the wall and inhibiting smooth muscle cell proliferation and migration (Corti and Badimon, 2002). The middle layer is the media which is the muscular part of the wall, containing smooth muscle cells, collagen and elastin. The outer layer is the adventitia which contains fibrous tissue (making it much stiffer than the media) and tethers the artery to the perivascular tissue.

When atherosclerosis occurs, a plaque consisting of lipid and fibrous tissue forms inside the intima layer of the artery wall (Libby, 2000; Yuan et al., 2000). Atherosclerosis is the most common arterial disease and can lead to heart attacks and strokes, making it the leading cause of death in the Western world. As the plaque grows the artery wall thickens; a large plaque may greatly reduce the lumenal area, reducing the blood flow and resulting in insufficient oxygen being obtained by the tissues downstream (ischemia).

One clinical procedure to increase or maintain the lumen is percutaneous translumenal coronary angioplasty (PTCA) where a wire object called a stent, shown in Figure 1(a), is placed inside the vessel to provide an internal scaffold to hold the walls apart. The wire stent is mounted on to a balloon catheter, Figure 1(b). During surgery the catheter is used to manoeuvre the stent along the blood vessels, to the diseased artery. Once the stent has been positioned at the site of the atherosclerotic plaque the balloon is inflated, causing the stent to expand in diameter and push the artery walls apart, as illustrated in Figure 1(c). The balloon is then removed, leaving the stent in situ as a permanent implant, increasing the area of the lumen, Figure 1(d). By relieving the blockage of the artery in this manner blood flow and oxygen transport to the tissues downstream are improved, reducing the likelihood that the patient will suffer from a heart attack or stroke.

The insertion of a stent causes some damage to the vessel and often the endothelium is removed during the process and the stent contacts the smooth muscle cells of the artery's media layer. Until the endothelium grows back, over a period of about four weeks, the endothelium's ability to inhibit smooth muscle cell proliferation is lost and the vessel wall may thicken over

the stent and reduce the lumenal area, a process called restenosis. The stent provokes an inflammatory response, which causes factors to be released which could also encourage tissue growth and restenosis. The high incidence of restenosis is a huge disadvantage of this clinical technique and often an atherosclerotic vessel must be stented several times before a suitably wide lumen is obtained.

To reduce restenosis after PTCA drugs such as paclitaxel and rapamycin can be mixed with a polymer and coated on to the stent (Alexis et al., 2004). These drugs diffuse into the artery wall where they are taken up by the smooth muscle cells. The drugs interrupt their cell cycle and thus prevent their proliferation. This is a recent technique however and we lack knowledge of which factors affect its success. Clinicians would like to obtain a uniform drug distribution over the arterial wall, however the arterial wall morphology, stent design and physiochemical properties of the drug are likely to affect the drug distribution obtained by the cells (Sousa et al., 2003). By mathematically modelling the drug transport across the artery wall, the subsequent uptake by the cells, and the effect of this upon the tissue growth, we hope to gain insight into the effectiveness of drug coated stents in preventing restenosis.

2 Review of mathematical models

In modelling the release of drug from arterial stents, and its impact on restenosis, a number of issues must be considered. A comprehensive modelling treatment would aim to couple haemodynamics, cell proliferation and drug diffusion through both the stent's polymer coating and the different layers of the artery wall. At present, such a complete treatment is still some way off. However, some insights have been gained through mathematical modelling of particular aspects of the problem. The aim of this section is to describe the main modelling issues, and discuss a few of the published models which have attempted to tackle them.

Drug transport across the artery wall occurs both by diffusion and convection with the blood plasma. From a fluid dynamic point of view, the artery wall may be treated as a porous medium, and hence the radial flow can be modelled using Darcy's law (Zunino, 2004). The anisotropic nature of the wall material means that the rate of diffusion of the drug may be different in different directions; for one particular type of drug, the planar and transmural diffusivities were found to differ by a factor of 45 (Hwang and Edelman, 2002). It may also be necessary to distinguish between solution (plasma) drug concentration and tissue drug concentration, as the hydrophobicity of some drugs may lead to preferential accumulation within the tissue. This effect is modelled by introducing a partition coefficient K, such that in steady state the cellular tissue drug concentration c_{T} is given by:

$$c_{\mathrm{T}} = K c_{\mathrm{E}}, \tag{1}$$

where c_{E} is the drug concentration in the extracellular fluid. In general, K may be concentration, space and time dependent (Hwang et al., 2003). Multi-region models may be employed to take account of the different drug transport properties of different regions of the arterial wall, and within the stent coating (Zunino, 2004).

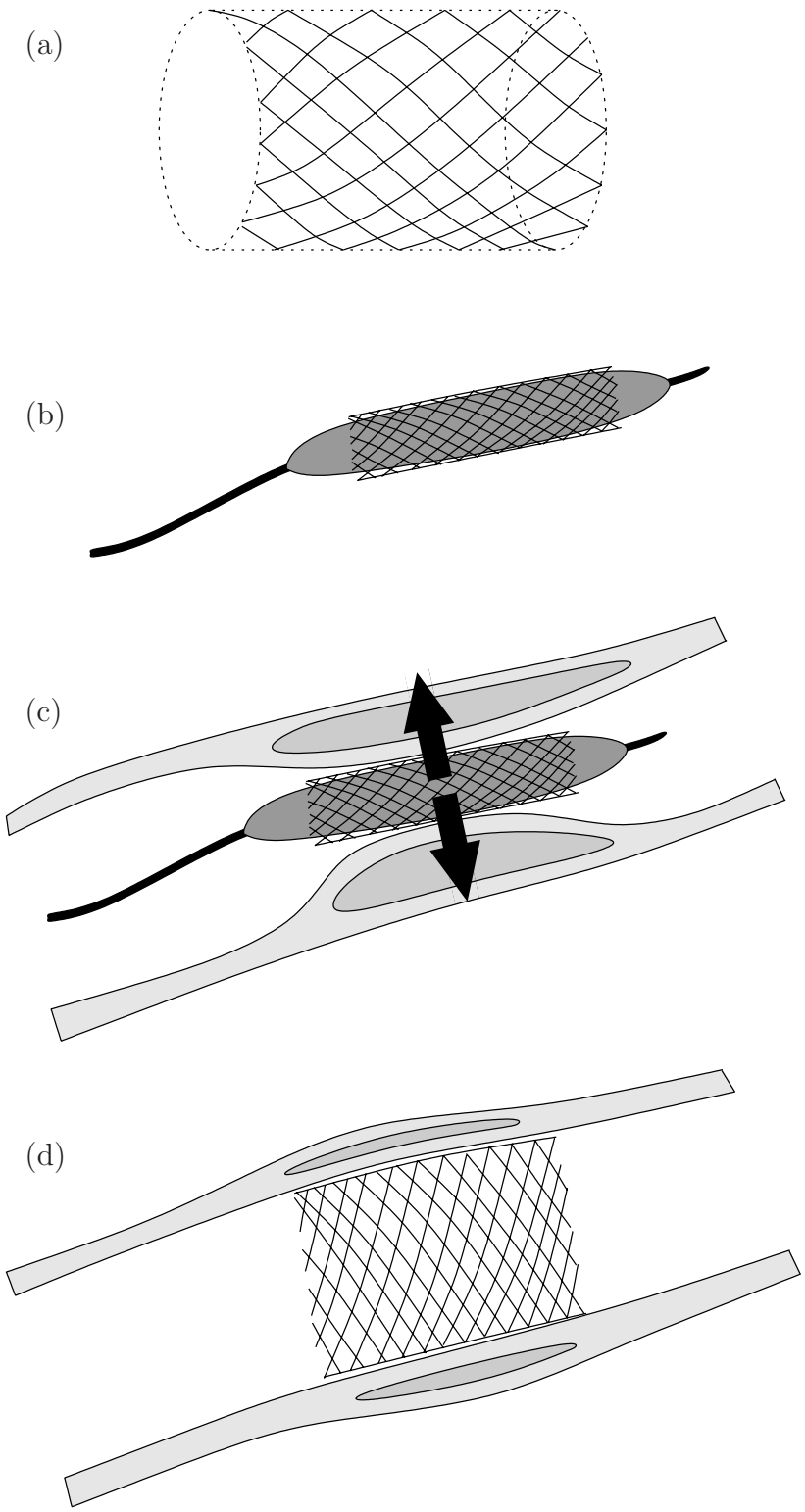

Figure 1: (a) A sketch of a wire mesh stent. (b) The tip of a balloon catheter, with a stent in compressed form mounted on the balloon. (c) A sketch showing the balloon catheter with stent in position at the site of an atherosclerotic plaque. Plaques cause a localised narrowing of the vessel which restricts blood flow. The arrows indicate direction of the expansion of the balloon. (d) The stent, after balloon inflation and catheter withdrawal. The stent holds open the lumen of the artery.

Clinically, several different designs of stent are used for implantation into patients. The stents are generally constructed of a wire mesh; however, the design of the mesh varies between stents. These design differences can affect the haemodynamics close to the artery wall, and lead to regions of unusually low or high wall shear stress (WSS). Low WSS is correlated with thrombus formation, whilst high stress may damage blood cells and cause platelet activation. In Montagano et al. (2003), computational fluid dynamics is applied to studying the distribution of WSS for two particular stent designs, and the implications for the likelihood of restenosis. Their conclusions appear to agree with clinical data, which show a difference of about 4% in restenosis rates between the two designs.

3 Modelling drug release from an arterial stent

3.1 Material properties

The wires forming the stent are assumed to be cylindrical with radius $r_{\text{wire}} = 5 \times 10^{-5}\,\text{m}$, and coated with polymer to a thickness of $h = 10^{-5}\,\text{m}$. The drug is embedded in the polymer and is released by a diffusion process, assumed to be isotropic. The diffusivity of the drug within the stent coating, D_P, is dependent on the polymer used, but values cited in the literature are around $10^{-14}\,\text{m}^2\,\text{s}^{-1}$, with some reported values as low as $10^{-16}\,\text{m}^2\,\text{s}^{-1}$.

The drug will diffuse through the media, which has a thickness of around $d = 4 \times 10^{-4}\,\text{m}$ and a porosity of $\phi = 0.61$. The diffusion is noticeably anisotropic, with diffusivities in the longitudinal and circumferential directions of the order of $10^{-10}\,\text{m}^2\,\text{s}^{-1}$, while the diffusivity in the radial direction is of the order of $10^{-12}\,\text{m}^2\,\text{s}^{-1}$ or less. We also note that there is a fluid flow from the blood vessel lumen to the cells due to the difference between the arterial blood pressure and the fluid pressure in the surrounding tissues. This fluid flow has been measured to have a discharge (volume flux per unit area) of around $v = 10^{-8}\,\text{m}\,\text{s}^{-1}$.

One of the most popular drugs used to prevent restenosis is paclitaxel. The tissue binding properties of this drug are described by Levin et al. (2004), who conducted an experiment where specimens of artery tissue are placed in a bath containing a solution of paclitaxel at concentration $\bar{c}$. The tissue is left in the solution for a period of 60 hours, after which it is removed and analysed. The final concentration of drug in the artery wall tissue, $c_{\text{T}}^{\text{final}}$ is found on average to be 30 times the concentration $\bar{c}$. A more detailed analysis showed that the binding capacity K, defined to be the ratio of drug concentration at any point in the tissue to $\bar{c}$, varies from a range of 13–25 in the media to around 16–45 in the adventitia. In this report we will assume a representative value for the media of $K = 15$, such that

$$c_{\text{T}}^{\text{final}} \;=\; K\,\bar{c}, \quad \text{where} \quad K = 15. \tag{2}$$

A separate experiment cited in Levin et al. (2004) measures the concentration of drug in arterial samples placed in a bath of paclitaxel solution over a period of 72 hours. The drug concentration in the tissue sample, $c_{\text{T}}(t)$, is measured at regular intervals. The results compared to the final equilibrium value, $c_{\text{T}}^{\text{final}}$, obtained at 72 hours following a 12-hour steady-state period. The evolution of c_{T} can be described by a first order reaction kinetics model, in which the rate

of change of c_{T} is proportional to the distance from the equilibrium value,

$$\frac{d\,c_{\mathrm{T}}}{dt} \;=\; \alpha\left(c_{\mathrm{T}}^{\mathrm{final}} - c_{\mathrm{T}}\right). \tag{3}$$

Equation 3, subject to the initial condition $c_{\mathrm{T}}(0) = 0$, can be solved to show

$$\tilde{c}_{\mathrm{T}}(t) \;=\; c_{\mathrm{T}}^{\mathrm{final}}\left(1 - \mathrm{e}^{-\alpha t}\right). \tag{4}$$

Comparison of this model with the experimental data presented in Levin et al. (2004) shows good agreement. The rate constant α is found to be around $2 \times 10^{-5}\,\mathrm{s}^{-1}$.

3.2 Drug delivery model

Any attempt at modelling a problem of this kind will require an understanding of the diffusion of drug from the polymer-coated stent through to the blood vessel wall. We will therefore consider at first only this aspect of the problem, neglecting the smooth muscle cell proliferation. This simplification of the model is valid if the timescale for the drug transport is short compared with the timescale for muscle cell growth, which can be shown to be a reasonable assumption using experimental data.

The complicated physiology of the artery wall will be simplified to the geometry portrayed in Figure 2. We will only consider two domains through which the drug is assumed to diffuse, namely the polymer coating the wire, and the smooth muscle cells that comprise the media.

We suppose that the concentration of the drug in the polymer is denoted c_P. The transport of drug within the polymer is assumed to be dominated by diffusion, so that:

$$\frac{\partial c_P}{\partial t} \;=\; D_P\left(\frac{\partial^2 c_P}{\partial x^2} + \frac{\partial^2 c_P}{\partial y^2}\right) \tag{5}$$

in the polymer, where D_P is the diffusivity of the drug in the polymer.

We consider the media as a porous medium consisting of a cell phase and the extracellular fluid. We denote the concentration in the two phases by c_I (the cell phase) and by c_E (extracellular fluid). Drug transport through the extracellular fluid is assumed to occur through both convection (due to the fluid flow from the blood through the media, with discharge $\mathbf{u} = -v\mathbf{j}$) and (anisotropic) diffusion. We also assume that the drug is absorbed by the cells at a rate $Q(c_E, c_I)$, and that once the drug is attached to a cell, it does not diffuse through the cell. In the media, we therefore have:

$$\phi\frac{\partial c_E}{\partial t} - v\frac{\partial c_E}{\partial y} \;=\; D_x\frac{\partial^2 c_E}{\partial x^2} + D_y\frac{\partial^2 c_E}{\partial y^2} - Q \tag{6}$$

$$(1-\phi)\frac{\partial c_I}{\partial t} \;=\; Q \tag{7}$$

where ϕ is the porosity of the medium. Note that we have supposed that the velocity field is constant and unaffected by the presence of the stent, which is physically unrealistic but avoids

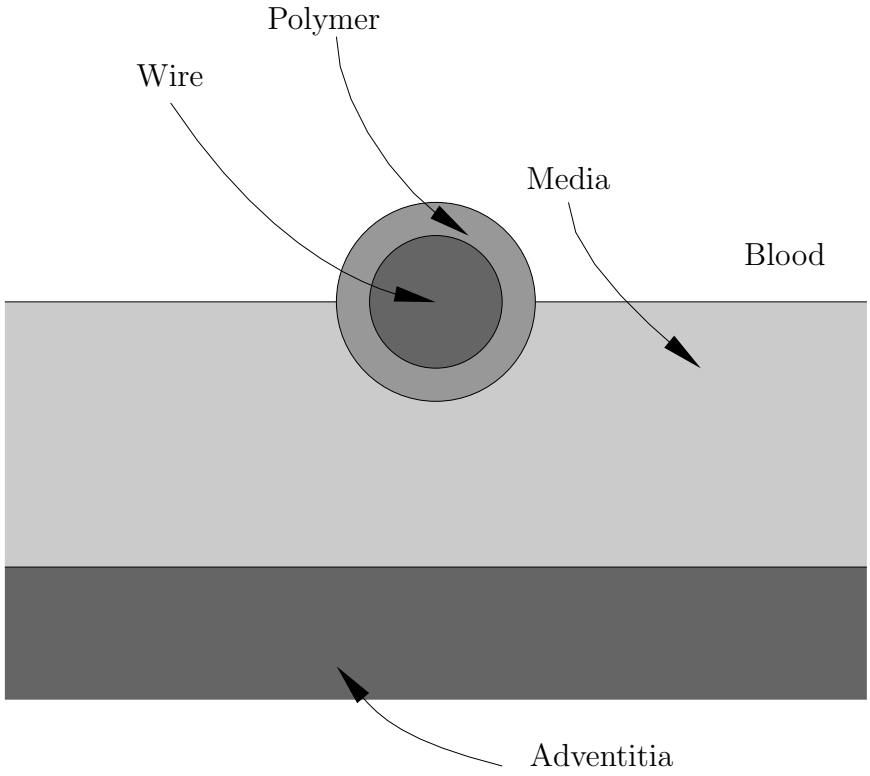

Figure 2: Simplified geometry of the two-dimensional model

the necessity of solving a fluid flow problem in the domain.

We choose:

$$Q = \alpha \left(c_E - \frac{c_I}{K} \right) \tag{8}$$

so that the rate at which the cells absorb the drug is proportional to the extracellular concentration initially, but that the ratio of internal concentration to extracellular concentration equilibrates to K.

The boundary conditions for the problem are, on the whole, intuitive. At the boundary between the polymer and the wire, we require zero flux of the drug into the impermeable metal wire. Where the polymer is in contact with the blood, any amount of drug reaching the bloodstream will be washed away by the relatively fast flowing blood. Therefore the concentration at the blood-polymer interface will be very low, and we impose the boundary condition $c_P = 0$ at this boundary. Similar considerations lead us to prescribe $c_E = 0$ at the boundary where the media is in contact with the blood. At the interface of the media and the polymer we impose continuity of extracellular drug concentration and polymer drug concentration, and also continuity of the corresponding fluxes of the drug. Accounting for both the adjective and diffusive

fluxes of the drug that are present in the media layer we find:

$$-D_P \frac{\partial c_P}{\partial y} = -D_y \frac{\partial c_E}{\partial y} - v\, c_E \quad \text{at} \quad y = 0. \tag{9}$$

At a distance ℓ away from the stent wire in the x-direction we should impose periodic boundary conditions. This is in order to model the fact that we have an array of wires, each releasing drug into the media. Finally, at the boundary between the media and the adventitia, we suppose that the flux of extracellular drug out of the media is proportional to the extracellular concentration at the boundary.

3.3 Scalings

In certain cases simplifications can be made to the above system of equations by considering the scalings of the different terms that result from nondimensionalisation of the model.

The timescale associated with a Brownian diffusion process is given by L^2/D, where L is a typical length scale and D is the relevant diffusivity. Thus, using the values in section 3.1, we obtain the following timescales for diffusion. For diffusion of the drug across the polymer layer, we obtain timescales between $10^4\,\mathrm{s}$ and $2 \times 10^5\,\mathrm{s}$, depending on the value used for the polymer diffusivity. Diffusion through the media occurs on a similar timescale, of $10^5\,\mathrm{s}$. The timescale for drug uptake by the cells has a representative value of $\alpha^{-1} = 5 \times 10^4\,\mathrm{s}$. The Peclet number $\mathrm{Pe} = Lv/D$ compares the flux of the drug due to diffusive processes with the convective flux, and is calculated for drug transport across the media to be $\mathrm{Pe}_{\mathrm{media}} = dv/D_x$, which is found to have a value of approximately 4. This shows that diffusive and advective fluxes of the drug in the media layer are of comparable size. Thus we find that, in the regime of clinical interest, the mathematical model cannot be simplified by neglecting terms that are small. Therefore, any simplifications made to the model need to be geometrical.

There is, however, one observation that we can make. By expressing equation (5), which describes diffusion within the polymer coating of the cylindrical wire, in polar coordinates and scaling $r = r_{\mathrm{wire}} + h\,R$, with $0 < R < 1$, to account for the thin geometry of the polymer layer, we find that the only significant diffusive term is $\partial^2 c_P/\partial R^2$. We thus conclude that most of the diffusion within the polymer occurs in the radial direction, and that any circumferential diffusion is insignificant. Therefore, the contact area of the wire and the artery wall will be highly important, since the only drug entering the wall will have originated from the part of the stent in contact with the wall; the rest will be washed away in the bloodstream. However, the mechanics of this contact problem are so complicated that we believe the only accurate way of determining the contact area is by experimental observations.

3.4 One-dimensional model

The solution of the full two-dimensional model described in §3.2 is outside the scope of this report, and we restrict our attention to a one-dimensional version of the model. The configura-

tion of this model can be seen in Figure 3, and is similar to the simplified geometry employed in (Sakharov et al., 2002).

Figure 3: One-dimensional model configuration

The model in one dimension simplifies to

$$\frac{\partial c_P}{\partial t} = D_P \frac{\partial^2 c_P}{\partial y^2} \qquad y \in [0, h] \tag{10}$$

$$\phi \frac{\partial c_E}{\partial t} - v \frac{\partial c_E}{\partial y} = D_y \frac{\partial^2 c_E}{\partial y^2} - \alpha \left(c_E - \frac{c_I}{K} \right) \qquad y \in [-d, 0] \tag{11}$$

$$(1 - \phi) \frac{\partial c_I}{\partial t} = \alpha \left(c_E - \frac{c_I}{K} \right) \qquad y \in [-d, 0] \tag{12}$$

$$D_y \frac{\partial c_E}{\partial y} + v c_E = \beta c_E \qquad y = -d \tag{13}$$

$$c_P = c_E \qquad y = 0 \tag{14}$$

$$-D_P \frac{\partial c_P}{\partial y} = -D_y \frac{\partial c_E}{\partial y} - v c_E \qquad y = 0 \tag{15}$$

$$\frac{\partial c_P}{\partial y} = 0 \qquad y = h. \tag{16}$$

Theoretically, this set of equations can be solved by Laplace transforms, but the solution obtained in transform variables is much too difficult to invert. We therefore turn to a numerical method.

3.5 Numerical simulations

The one-dimensional model described in §3.4 was solved numerically using a simple finite difference scheme, implemented in Matlab. A numerically stable scheme for this advection-diffusion system was obtained using the fully-implicit backward Euler time-stepping method.

In the absence of data for the value of the parameter β, which occurs in the boundary condition (13) at the bottom of the media layer, $y = -d$, three cases were considered. Two limiting cases were examined in which the flux of the drug out of the media layer was (i) very slow, modelled by choosing $\beta = 0$, and (ii) very rapid, for which we consider the limit $\beta \to \infty$. A third value, $\beta = D_y/d$ was chosen to represent an intermediate case, in which the flux out of the media layer is comparable in magnitude with the diffusive fluxes present within the media.

Profiles of c_P, c_E and c_I, at regular time intervals between $t = 0\,\mathrm{s}$ and $t = 10^5\,\mathrm{s}$, are shown in Figure 4. The model is linear with respect to the concentrations, c_E, c_I and c_P, thus the results scale linearly with the initial drug concentration in the polymer. Therefore all concentrations are normalised by the initial drug concentration in the polymer at time $t = 0\,\mathrm{s}$, and all plots show the normalised concentration values. Profiles are shown for the three values of β discussed above and two values of α, the cellular drug uptake rate constant: the first value, $\alpha = 2 \times 10^{-5}\,\mathrm{s}^{-1}$, is derived from data in Levin et al. (2004) as described in §3.1, and a second set of results, which represent a more reactive drug with $\alpha = 2 \times 10^{-4}\,\mathrm{s}^{-1}$, are also shown. The other parameter values are the same as in §3.1:

$$\begin{aligned} D_P &= 1.0 \times 10^{-14}\,\mathrm{m^2\,s^{-1}}, \quad & D_y &= 1.0 \times 10^{-12}\,\mathrm{m^2\,s^{-1}}, \quad & h &= 1.0 \times 10^{-5}\,\mathrm{m}, \\ d &= 4.0 \times 10^{-4}\,\mathrm{m}, \quad & v &= 1.0 \times 10^{-8}\,\mathrm{m\,s^{-1}}, \quad & K &= 15, \quad & \phi &= 0.61. \end{aligned}$$

Figure 5 shows the time variation of the mass of drug within the polymer, extracellular fluid and the cells of the media layer. E.g. at time $t = 0$, all the drug is contained within the polymer, and none is present within the extracellular fluid or the cells. The total mass of the drug within the system is also shown. For $\beta \neq 0$, the total mass decreases with time as mass is lost to the lower layers of the artery wall.

We see in Figure 4 and 5 that the drug escapes rapidly from the polymer layer. The results show that a more reactive drug (with $\alpha = 2 \times 10^{-4}$) is initially better absorbed by the cells of the medial layer than the drug with lower reactivity. The fast absorption of the drug by the cells initially prevents the more reactive drug from being washed out of the system by the advective flux. This is shown by the *absence* in Figures 5(d),(f) of the rapid decrease in the total drug mass within the system by time $t = 0.5$ days which is clearly visible in figures 5(c),(e).

At longer times, $t > 2.5$ days, it appears that the cellular drug concentration is most strongly effected by β, which regulates the flux of the drug leaving the system. This is because our model describes reversible binding of the drug to the cells. Thus for large β, for which the extracellular drug is easily removed from the system, the low levels of c_E cause the drug to unbind from the cells more rapidly.

The concentration of the drug in cells near the surface of the media layer, $y = 0$, may be of clinical interest, as these cells may play a significant role in vessel restenosis. The time variation of this quantity is shown in Figure 6. We see that increasing the drug activity, α, leads to a considerable increase in the amount of drug absorbed at $y = 0$. The results for the concentration c_I at the surface $y = 0$ are found to be almost independent of the flux parameter β.

4 Modelling restenosis

In this section, we shall investigate models for the proliferation of smooth muscle cells (SMC) in a stented artery, and the resulting restenosis of the vessel.

4.1 Model formulation - tissue growth

We assume the artery is an axisymmetric tube, of which we consider a two-dimensional cross-section. The lumen of the vessel is assumed to have radius $a(t)$, whilst the radius of the vessel up to the media / adventitia interface is R^* (taken as constant). As a simplification, we shall treat the stent as a hoop, of radius R_s. We shall now develop a model for the proliferation of the smooth muscle cells in the artery wall, based on the tumour growth model of Franks and King (Franks and King, 2003; King and Franks, 2004). We let n be the volume fraction of SMCs within the intima, and ρ is taken to be the volume fraction of cellular debris and extracellular fluid. We assume there are no voids, so that:

$$n + \rho = 1. \tag{17}$$

We let the concentration of drug be c (equations describing its transport within the layer of proliferating cells will be derived in §4.2). Both cells and cellular debris / fluid are assumed to move with the same velocity $\boldsymbol{v}$; cells proliferate at a rate $g(n, c)$ and die at a rate $f(n, c)$, whence they become part of the cellular debris phase. Cellular debris is removed, *e.g.* by the immune system, at a rate $h(n, c)$. Our governing equations are then:

$$\frac{\partial n}{\partial t} + \nabla \cdot (n\boldsymbol{v}) = g(n, c) - f(n, c), \tag{18}$$

$$\frac{\partial \rho}{\partial t} + \nabla \cdot (\rho\boldsymbol{v}) = f(n, c) - h(n, c). \tag{19}$$

We note that, by adding the two equations above, we obtain:

$$\nabla \cdot \boldsymbol{v} = g - h. \tag{20}$$

In general, this equation would require a constitutive relation to close the system (*e.g.* Darcy's law, or Stokes' law); however, this is not necessary in the one-dimensional case which follows.

4.1.1 Drug-free case: uniform proliferation

We restrict our attention to the one-dimensional axisymmetric case, and assume that the volume fraction of cells (and hence cellular debris) remains constant within the artery wall. We take the

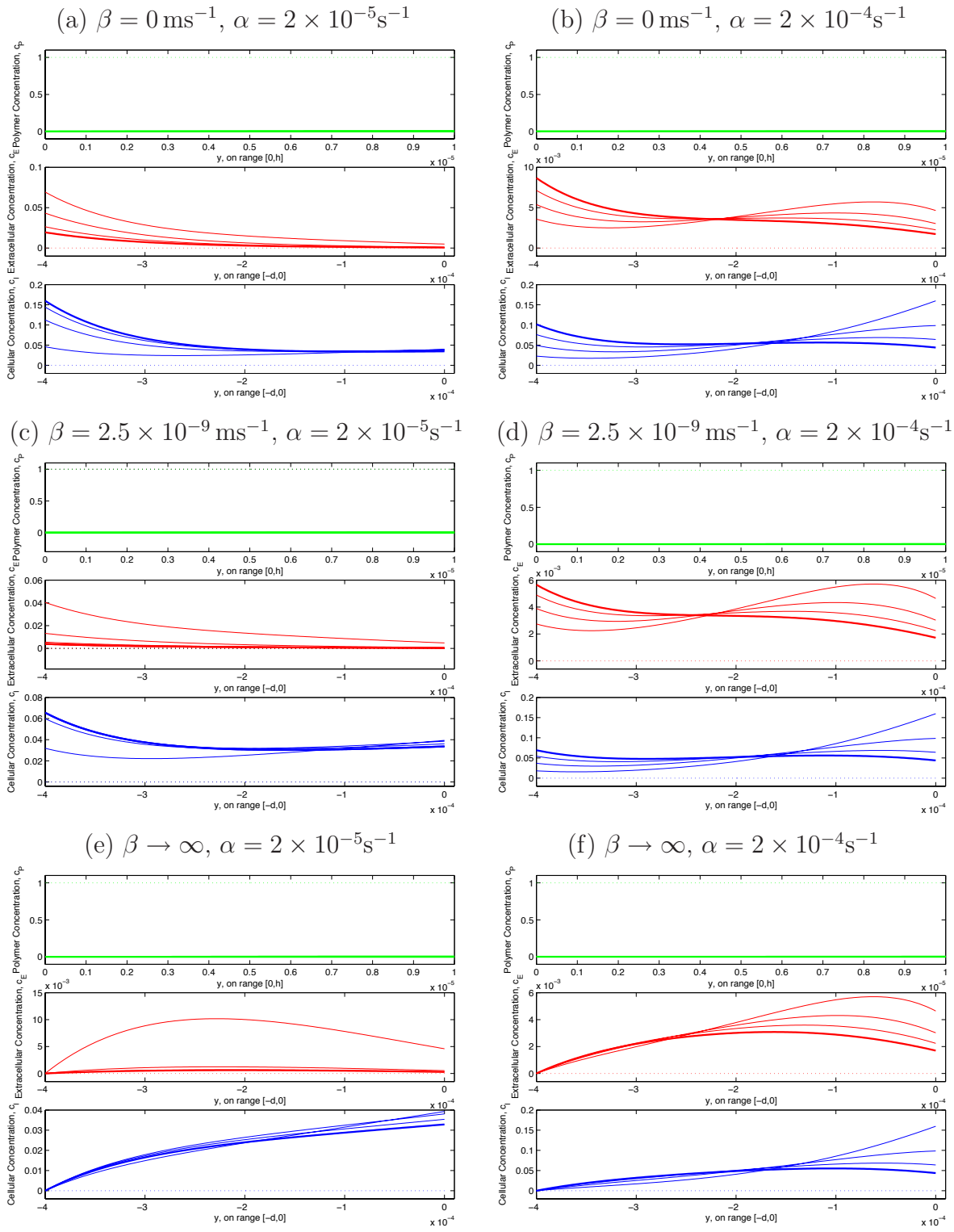

Figure 4: Solutions of the one-dimensional model for 3 values of β and two values of α. Each of the 6 subplots shows the concentration in the polymer, c_P on $y \in [0, h]$ (top graphs), the extracellular concentration, c_E on $y \in [-d, 0]$ (middle graphs) and the cellular concentration, c_I, on $y \in [-d, 0]$ (lower graphs). The upper surface of the media layer is located at $y = 0$. In each plot, the initial conditions are shown by dotted lines, and the final solution at $t = 1 \times 10^5$s is shown by the thicker line. Other parameter values are described in the text. *Note that in order to show the individual solutions clearly, the axis scales vary between plots.*

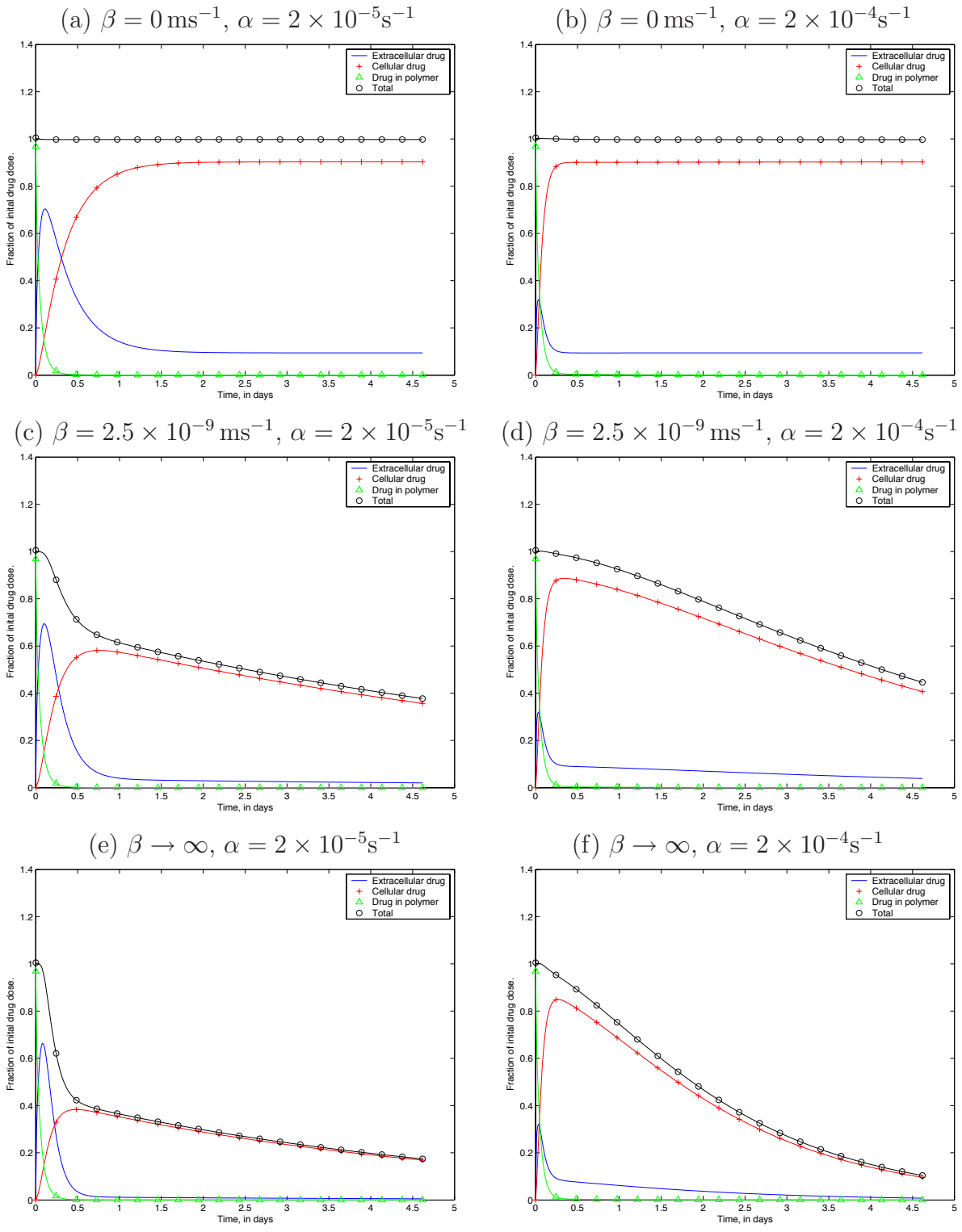

Figure 5: Time variation in the drug distribution for the one-dimensional model for 3 values of β and two values of α. Each of the 6 subplots shows variation of the overall mass of drug contained in the polymer, extracellular fluid and within the cells of the tissue for times between 0 to 4.5 days. The time variation of the total mass of the drug within the system is strongly effected by the value of β, which determines the boundary condition at $y = -d$.

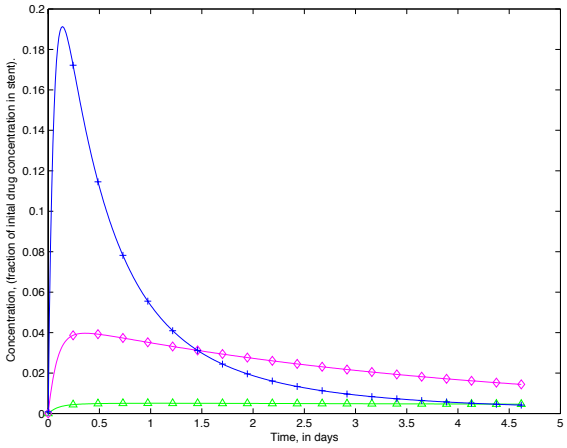

Figure 6: Time variation of the drug concentration at the surface of the media layer, $y = 0$ for three values of α with $\beta = D_y/d$. Quantitatively similar results were obtained for $\beta = 0$ and $\beta \to \infty$. The graph shows results for $\alpha = 2 \times 10^{-6}\,\mathrm{s}^{-1}$ (green line, marked with triangles), $\alpha = 2 \times 10^{-5}\,\mathrm{s}^{-1}$ (pink line, marked with diamonds), and $\alpha = 2 \times 10^{-4}\,\mathrm{s}^{-1}$ (blue line, marked with + signs).

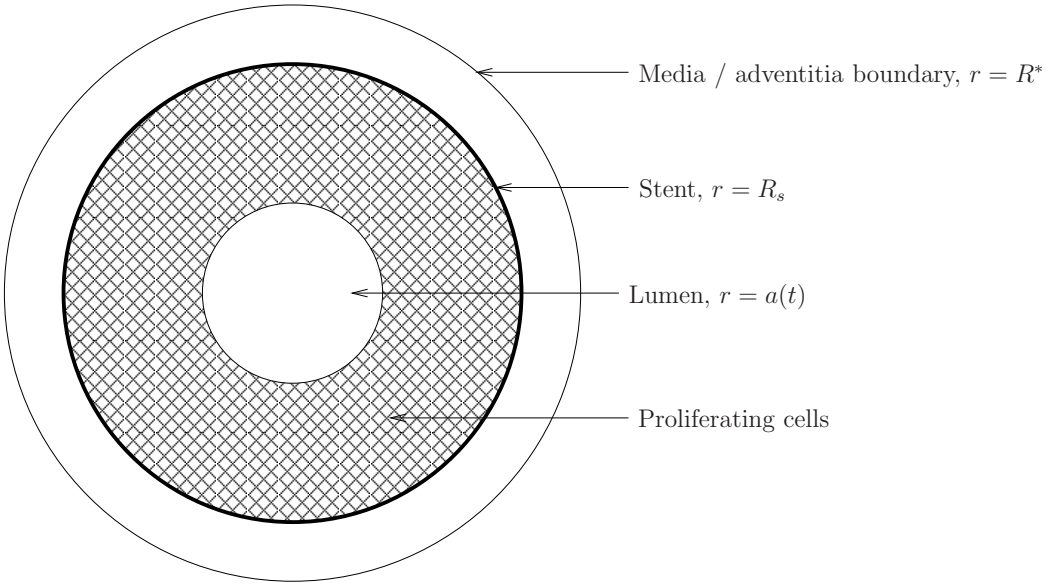

Figure 7: Definition sketch

volume fraction of cells to be n_0, and assume that there is a constant rate of cell proliferation and removal of extracellular debris. We hence adopt the following forms for g and h:

$$g = \alpha_1 n_0, \qquad h = \beta_1(1 - n_0). \tag{21}$$

Our model then reduces to:

$$\frac{1}{r}\frac{\partial(rv)}{\partial r} = \lambda, \tag{22}$$

where v is the radial velocity of the cells and $\lambda = g - h$. (Note that, in this case, we do not need to specify a form for f). We also observe that a steady state (*i.e.* $v = 0$) of equation (22) exists, in which $n_0 = \beta_1/(\alpha_1 + \beta_1)$. This represents the normal balance between cell proliferation and removal of cellular debris which is maintained in the presence of the endothelium. However, when the endothelium is removed, the rate of cell proliferation increases, and this balance is destroyed.

Equation (22) is subject to the following boundary conditions:

$$v = 0 \text{ on } r = R^*, \qquad v = \frac{da}{dt} \text{ on } r = a. \tag{23}$$

We now nondimensionalise the model, scaling lengths with R_s and time with λ^{-1}:

$$\tilde{r} = \frac{r}{R_s}, \ \tilde{t} = \lambda t, \ \tilde{v} = \frac{v}{R_s\lambda}, \ \tilde{a} = \frac{a}{R_s}, \tag{24}$$

to obtain the following equation and boundary conditions (dropping tildes):

$$\frac{1}{r}\frac{\partial(rv)}{\partial r} = 1, \tag{25}$$

$$v = 0 \text{ on } r = R, \qquad v = \frac{da}{dt} \text{ on } r = a. \tag{26}$$

where $R = R^*/R_s$.

Integrating equation (25) once, and imposing the boundary condition on $r = R$ gives:

$$v = \frac{1}{2}\left(r - \frac{R^2}{r}\right). \tag{27}$$

We can now solve for the free boundary $a(t)$, which defines the radius of the lumen, as this obeys the following ODE:

$$\frac{da}{dt} = \frac{1}{2}\left(a - \frac{R^2}{a}\right), \tag{28}$$

subject to the initial condition that $a(0) = 1$ - *i.e.* just after the stent is implanted, the radius of the lumen is the same as that of the stent. Hence:

$$a^2 = R^2 + (1 - R^2)e^{2t} \tag{29}$$

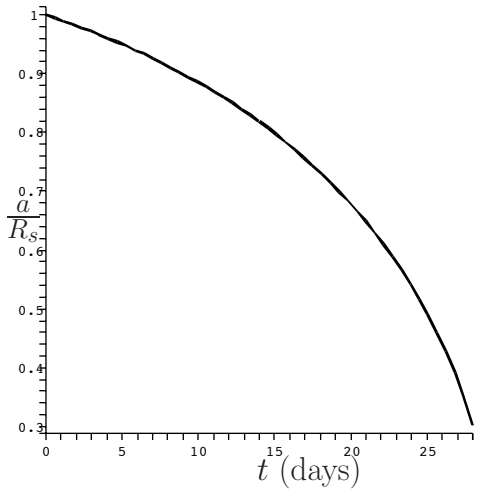

Figure 8: Restenosis in the absence of drug

Our model thus predicts that the artery will become completely blocked after a time t_b, given by:

$$t_b = \frac{1}{2} \log \frac{R^2}{R^2 - 1}. \tag{30}$$

This is clearly an unrealistic prediction, because as the artery becomes increasingly stenosed, the blood pressure will rise, compressing the wall tissue and hence our assumption of constant cell volume fraction may become invalid. However, t_b gives us a rough timescale over which we can expect the stenosis to become severe in untreated cases.

Our model may, however, provide a reasonable description of the earlier stages of restenosis. Using information from Buergler et al. (2000), which studied restenosis in pigs, we note that after 28 days, the lumenal diameter decreases by about 70% (*i.e.* $a \approx 0.3R_s$) and the average value of the ratio $R^*/R_s = 1.2$. Substituting these values into our equation for a above, we find a value for the parameter λ, of around 0.02 day^{-1}. A plot of the dimensionless lumen radius for the above parameter values is shown in Figure 8.

4.2 Drug diffusion within the media tissue

We now turn to modelling the distribution of the drug within the new wall tissue - *i.e.* the region $a(t) \leq r \leq R_s$. In order to keep our model as simple as possible, we will assume that diffusion, with coefficient D, is the dominant transport mechanism (this may in practice be a poor approximation, see §3.3). The drug will both decay naturally, and also be taken up by the cells; hence we postulate a sink term of the form $(c_1 + c_2 n_0)c$, where c_1 and c_2 are constants, and n_0 is the volume fraction of live cells (as before, assumed constant). If we make the further assumption that the timescale of drug diffusion is much shorter than that for tissue growth (not unreasonable, given the drug diffusion timescale stated in §3.3 and the value of λ calculated

above) we arrive at the following equation for c:

$$\frac{\partial^2 c}{\partial r^2} + \frac{1}{r}\frac{\partial c}{\partial r} - \sigma^* c = 0, \tag{31}$$

where $\sigma^* = \frac{(c_1 + c_2 n_0)}{D}$. This is subject to the following boundary conditions:

$$c(R_s) = c_s, \qquad c(a) = 0, \tag{32}$$

which represent a constant drug concentration at the stent, and zero drug concentration in the blood. As was explained in §3.2, the boundary condition at $r = a$ is realistic, as the blood will 'wash away' any drug reaching the lumen. However, the condition at $r = R_s$ is an idealisation, representing the case in which the stent coating contains a great deal of drug, and the polymer coating controls its release so as to give a constant drug concentration at the stent surface. In practice, we would expect c_s to vary in time, and a more complete treatment would model the stent as an additional layer, as in the model of §3.2, coupling drug transport through the stent coating to transport in the artery wall.

We now nondimensionalise this model using the same scalings as above, supplemented by $\tilde{c} = \frac{c}{c_s}$. The governing equation and boundary conditions are now (dropping tildes):

$$\frac{\partial^2 c}{\partial r^2} + \frac{1}{r}\frac{\partial c}{\partial r} - \sigma c = 0, \tag{33}$$

$$c(1) = 1, \qquad c(a) = 0, \tag{34}$$

where $\sigma = \sigma^* R_s^2$.

The solution to the above may be found in terms of modified Bessel functions:

$$c(r) = AI_0(\sqrt{\sigma} r) + BK_0(\sqrt{\sigma} r), \tag{35}$$

where A and B are constants obeying:

$$AI_0(\sqrt{\sigma} a) + BK_0(\sqrt{\sigma} a) = 0, \quad AI_0(\sqrt{\sigma}) + BK_0(\sqrt{\sigma}) = 1. \tag{36}$$

Equation (33) will also apply in the region between the stent and the adventitia (*i.e.* $1 < r < R$ in nondimensional terms), with the following boundary conditions:

$$c(1) = 1, \qquad \frac{\partial c}{\partial r}|_{r=R} = -\kappa c(R), \tag{37}$$

where κ represents the flux of drug into the adventitia.

The solution is hence:

$$c = PI_0(\sqrt{\sigma} r) + QK_0(\sqrt{\sigma} r), \tag{38}$$

and, on applying the boundary conditions, we find that P and Q obey:

$$PI_0(\sqrt{\sigma}) + QK_0(\sqrt{\sigma}) = 1, \tag{39}$$

$$\sqrt{\sigma}\left(PI_1(\sqrt{\sigma} R) - QK_1(\sqrt{\sigma} R)\right) = -\kappa\left(PI_0(\sqrt{\sigma} R) + QK_0(\sqrt{\sigma} R)\right) \tag{40}$$

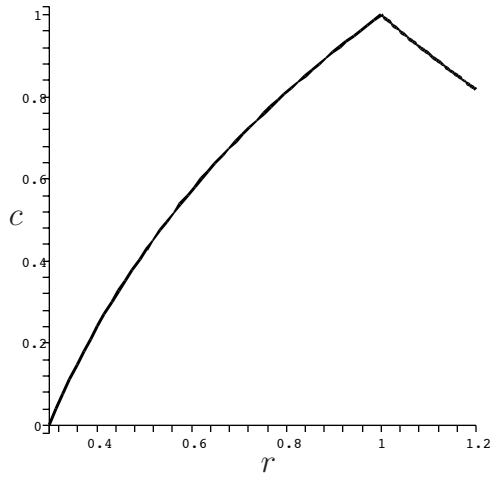

Figure 9: Drug concentration within the artery wall ($\kappa = 1$, $\sigma = 0.1$, $a = 0.3$, $R = 1.2$)

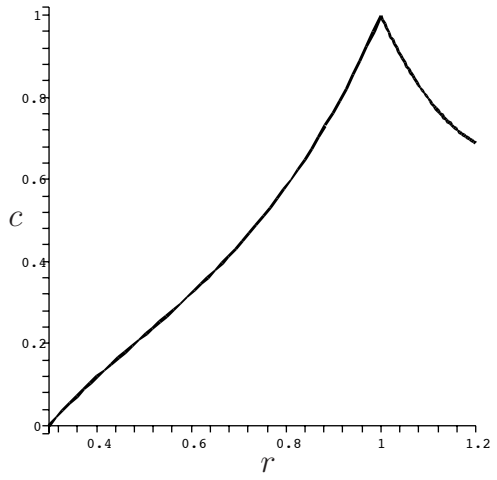

Figure 10: Drug concentration within the artery wall ($\kappa = 1$, $\sigma = 10$, $a = 0.3$, $R = 1.2$)

We recall from §3.1, that the uptake rate for the drug by the cells α is $O(10^{-5}s^{-1})$ and the radial diffusion coefficient $D \sim 10^{-12}m^2s^{-1}$; from (Buergler et al., 2000), we take $R_s \sim 10^{-3}m$. We hence estimate σ using the quantity $\alpha R_s^2/D$ as being approximately 0.1. The parameter κ, which specifies the flux of drug from the media into the adventitia cannot be estimated from the literature, so we shall take $\kappa = 1$. We can thus plot the distribution of the drug for given values of a; when $a = 0.3$, and other parameters take the values mentioned above, the solution is as displayed in Figure 9. The effect of increasing the rate of drug consumption / decay (to $\sigma = 10$) is to give a distribution which is more strongly peaked close to the stent, as shown in Figure 10.

4.2.1 Drug present case: inhibition of cell proliferation

We now return to our model of section §4.1, modifying the equations to include the effect of the drug as an inhibitor of cell proliferation. Thus, the term $g(n, c)$ now becomes:

$$g(n, c) = \frac{\alpha_1 n_0}{1 + kc}, \tag{41}$$

where k is a constant which describes the 'potency' or 'efficacy' of the drug at inhibiting cell proliferation. Note that we still retain the simplifying assumption that the volume fraction of cells is constant.

In the previous section, we found the solution for the drug distribution within the media in terms of Bessel functions. However, if we were to substitute this solution into equation (22), we would be unable to make any analytical progress. Instead, we shall attempt to gain some qualitative insights by using linear approximations of the drug concentration profiles. In the

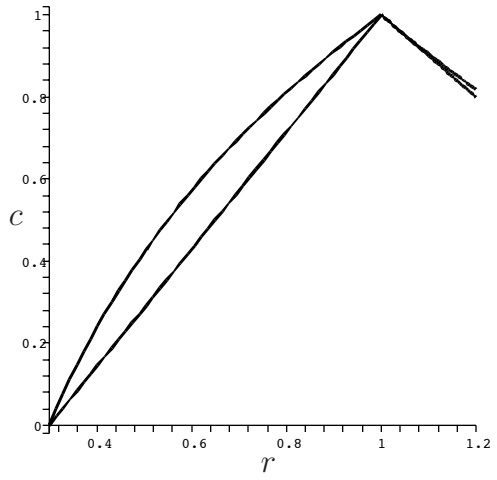

Figure 11: Exact and approximate solutions for c ($\kappa = 1$, $\sigma = 0.1$, $a = 0.3$)

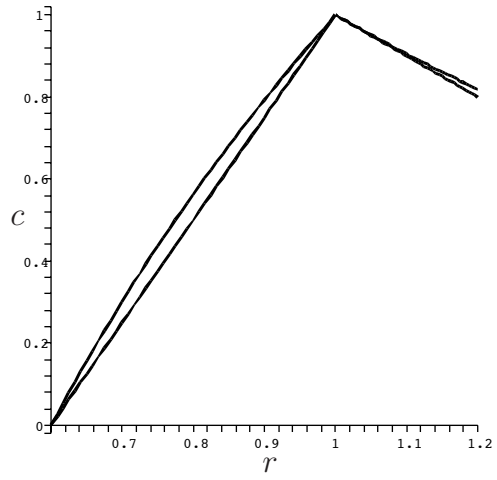

Figure 12: Exact and approximate solutions for c ($\kappa = 1$, $\sigma = 0.1$, $a = 0.6$)

region $a(t) < r < 1$ (in dimensionless variables), we approximate $c(r)$ by the line:

$$c = \frac{r - a}{1 - a}, \tag{42}$$

where we have scaled concentrations with c_s and lengths with R_s, as before. Similarly, in the region $1 < r < R^*$, we approximate c using the line:

$$c = 2 - r \tag{43}$$

In Figures 11 and 12 we show the exact and approximate solutions for c for two values of a ($a = 0.3$ and $a = 0.6$ respectively). We see that, for the parameter values chosen, the linear functions provide a reasonable approximation of the true solutions.

We now nondimensionalise equation (22), incorporating the new form for g (41) and the linear approximation for c. We introduce a new scaling for the time, based on cell proliferation in the drug free case (as the drug inhibits cell proliferation, this scaling is more convenient in this case). Thus, we set $\tilde{t} = \alpha_1 n_0 t$ and $\tilde{v} = v/\alpha_1 n_0 R_s$, but the length and concentration scalings remain unchanged from §4.2. We hence obtain:

$$\frac{1}{r}\frac{\partial(rv)}{\partial r} = \frac{1 - a}{1 - k_1 a + k_2 r} - \beta_2, \quad \text{in } a < r < 1 \tag{44}$$

where $k_2 = kc_s$ and $\beta_2 = \beta_1(1 - n_0)/\alpha_1 n_0$ are dimensionless parameters. These represent the effectiveness of the drug (a combination of its concentration and potency) and the relative rate of clearance of cellular debris respectively. For algebraic convenience, we have also introduced $k_1 = 1 + k_2$.

$$\frac{1}{r}\frac{\partial(rv)}{\partial r} = \frac{1}{\delta - k_2 r} - \beta_2, \quad \text{in } 1 < r < R \tag{45}$$

where we have introduced $\delta = 1 + 2kc_s = 1 + 2k_2$ for algebraic convenience.

Integrating the equation (44), we obtain:

$$v = \frac{1-a}{r}\left(\frac{r}{k_2} - \frac{(1-k_1 a)\ln(1-k_1 a + k_2 r)}{k_2^2}\right) - \frac{\beta_2 r}{2} + \frac{C_2(t)}{r} \text{ in } a(t) < r < 1, \quad (46)$$

where $C_2(t)$ is determined by imposing continuity of v at $r = 1$. Integration of equation (45), and imposition of the boundary condition $v(R) = 0$ gives:

$$v = \frac{1}{k_2}\left(\frac{R}{r} - 1\right) + \frac{\delta}{r k_2^2}\ln\left(\frac{\delta - k_2 R}{\delta - k_2 r}\right) + \frac{\beta_2}{2}\left(\frac{R^2}{r} - r\right) \text{ in } 1 < r < R, . \quad (47)$$

Imposing continuity of v at $r = 1$, we thus find that:

$$C_2 = \frac{1}{k_2}(R-1) + \frac{\delta}{k_2^2}\ln\left(\frac{\delta - k_2 R}{\delta - k_2}\right) + \frac{\beta_2 R^2}{2} - (1-a)\left(\frac{1}{k_2} - \frac{(1-k_1 a)\ln((1-a)(1+k_2))}{k_2^2}\right) \quad (48)$$

Now we impose the free-surface condition, $\frac{da}{dt} = v|_{r=a}$, choosing v according to whether $a < 1$ or $a > 1$. We then obtain the following pair of nonlinear equations which describe the evolution of the lumen diameter a:

$$\frac{da}{dt} = \frac{1}{k_2}\left(\frac{R}{a} - 1\right) + \frac{\delta}{a k_2^2}\ln\left(\frac{\delta - k_2 R}{\delta - k_2 a}\right) + \frac{\beta_2}{2}\left(\frac{R^2}{a} - a\right) \text{ for } a > 1 \quad (49)$$

$$\frac{da}{dt} = \frac{1-a}{a}\left(\frac{a}{k_2} - \frac{(1-k_1 a)\ln(1-a)}{k_2^2}\right) - \frac{\beta_2 a}{2} + \frac{C_2(a)}{a}, \text{ for } a < 1 \quad (50)$$

We now wish to consider steady state solutions for a. First, we look for such solutions with $a > 1$ - *i.e.* cases in which the cells do not grow over the stent following implantation. By inspection of equation (49), it is clear that $a = R$ is one such solution. As we have found that $R = 1.2$ is a representative value from experimental data, we can use the approximation that $R - a$ is small in this case to expand the logarithm term as a power series, retaining only the first term. We hence obtain the following equation for the steady state values of a:

$$(R-a)\left(1 - \frac{\delta}{\delta - k_2 a} + \frac{\beta_2 k_2 (R+a)}{2}\right) = 0. \quad (51)$$

The part of the equation in brackets can be re-written as the following quadratic for a:

$$a^2 + a\left(\frac{2}{\beta_2 k_2} - \frac{1}{k_2}(k_2 R - \delta)\right) + \frac{R\delta}{k_2} = 0. \quad (52)$$

For $R = 1.2$, we see that both the coefficient of a and the constant term in the above equation will be positive; this implies the two roots of the equation are negative, and hence are not physically realisable. We conclude that the only physically realisable steady state solution for which $a > 1$ is $a = R$. This is confirmed by performing numerical simulations of equations (49) in Maple, the results of which are shown in Figure 13. Increasing the effectiveness of the drug k_2 reduces the time taken to reach the steady state, as does increasing the clearance rate

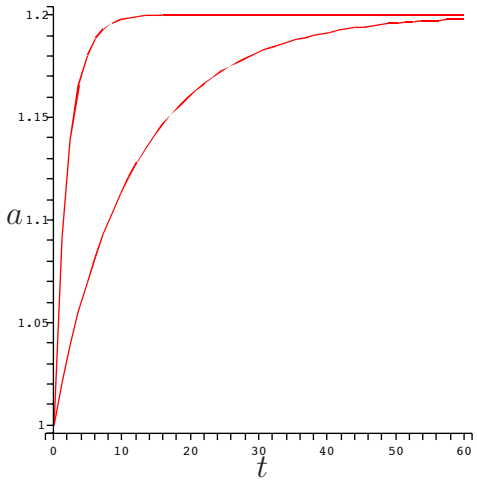

Figure 13: Evolution of lumen diameter with $R = 1.2$, $\beta_2 = 1$ and $k_2 = 1$ (upper curve), $k_2 = 0.1$ (lower curve)

of cellular debris, β_2. However, if k_2 or β_2 are too small (*i.e.* the drug has little effect on cell proliferation, or cellular debris is allowed to accumulate), we find that a will decrease below unity, and we must hence turn to equation (50).

Numerical simulations of equation (50) are displayed in Figure 14. We see that increasing the effectiveness of the drug significantly reduces the rate of restenosis. A similar effect is noted for increasing β_2. Although, in this regime, total restenosis is eventually predicted by our model, in reality, the reduction in the rate of SMC proliferation would afford an opportunity for the endothelial lining of the artery to regrow, which would, we expect, prevent further restenosis.

5 Conclusions

In this report, we have described the development of models treating two problems related to the introduction of a stent into an artery. In §3, we considered at the release of a drug from a polymer coated stent. Simple scaling arguments, described in §3.3 suggest that the proportion of the drug which is absorbed by the artery wall is dependent on the precise contact area between each wire of the stent and the underlying tissue. Because the contact problem requires detailed knowledge of the local biomechanics of a diseased artery wall, and knowledge of the mechanical forces applied during stent insertion, it seems unlikely that mathematical modelling can provide satisfactory results for this contact problem. However, the transport of the drug within the artery wall is quite amenable to mathematical modelling.

We established a simple model describing the advection and diffusion of the drug and its uptake by cells in the media layer of the artery wall. We solved this model in a simplified one dimensional geometry. We found that the initial release of a drug from a drug coated stent, over times <2.5 days after stent insertion, is governed by the drug's cell binding properties. At

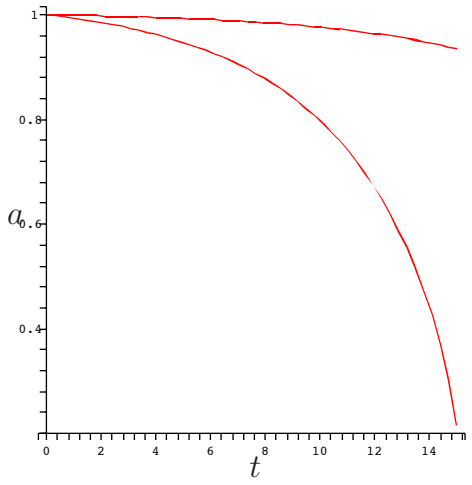

Figure 14: Evolution of lumen diameter with $R = 1.2$, $\beta_2 = 0.5$ and $k_2 = 1.1$ (upper curve), $k_2 = 1.0$ (lower curve)

later times, variation in the cellular drug concentration is largely accounted for by the transport of the drug to the outer layer of the artery wall. Future work could include the study of more complex geometries and more complex drug-cell binding kinetics. We note that several published studies, listed in §2, have already made progress in these areas.

In §4.1, we treated the related problem of smooth muscle cell proliferation in a stented artery, which can lead to restenosis. We showed, using our simple model, that drug-eluting stents can slow the rate of restenosis, or possibly eliminate the problem altogether, if the drug is sufficiently effective (in practice, there will be issues of toxicity, which we have not considered here). One of the most significant limitations of this model was the assumption of a constant drug concentration on the surface of the stent. We described how a more complete treatment would include coupling of drug transport within the stent coating to that in the artery wall, as in the model of §3.2. Another limitation was the neglect of drug convection with the transmural fluid flow, which, again was included in the model of §3.2. Such extensions are left to future work.

References

F. Alexis, S. S. Venkatraman, S. K. Rath, and F. Boey. In vitro study of release mechanisms of paclitaxel and rapamycin from drug-incorporated biodegradable stent matrices. *Journal of controlled release*, 98:67–74, 2004.

J. M. Buergler, F. O. Tio, D. G. Schulz, M. M. Khan, W. Mazur, B. A. French, A. E. Raizner, and N. M. Ali. Use of nitric-oxide-eluting polymer coated coronary stents for prevention of restenosis in pigs. *Coronary Artery Disease*, 11:351–357, 2000.

R. Corti and J. J. Badimon. Biological aspects of vulnerable plaque. *Current Opinion in Cardiology*, 17:616–625, 2002.

S. J. Franks and J. R. King. Interactions between a uniformly proliferating tumour and its surroundings: uniform material properties. *Math. Med. Biol.*, 20(1):47–89, 2003.

C.-W. Hwang and E. R. Edelman. Arterial ultrastructure influences transport of locally delivered drugs. *Circulation Research*, 90:826–832, 2002.

C.-W. Hwang, D. Wu, and E. R. Edelman. Impact of transport and drug properties on the local pharmacology of drug-eluting stents. *International Journal of Cardiovascular Interventions*, 5:7–12, 2003.

J. R. King and S. J. Franks. Mathematical analysis of some multi-dimensional tissue-growth models. *Euro. J. App. Math.*, 15:273–295, 2004.

A.D. Levin, N. Vukmirovic, C.-W. Hwang, and E.R. Edelman. Specific binding to intracellular proteins determines arterial transport properties for rapamycin and paclitaxel. *Proceedings of the National Academy of Sciences of the USA*, 101(25):9463–9467, 2004.

P. Libby. Changing concepts of atherogenesis. *Journal of Internal Medicine*, 247:349–358, 2000.

V. Montagano, S. Morosi, M. Dayar, A. Gomma, M. Atherton, M. Collins, and A. Redaelli. The link between restenosis and cardiovascular stent design: a study combining compuational fluid dnamics with computer aided design. *Internal Medicine*, 11:14–23, 2003.

D. V. Sakharov, L. V. Kalachev, and D. C. Rijken. Numerical simulation of local pharmacokinetics of a drug after intravascular delivery with an eluting stent. *Journal of Drug Targeting*, 10(6):507–513, 2002.

J. E. Sousa, P. W. Serruys, and M. A. Costa. New frontiers in cardiology. drug-eluting stents: part i. *Circulation*, 107:2274–2279, 2003.

X. M. Yuan, U. T. Brunk, and L. Hazell. The morphology and natural history of atherosclerosis. In Dean R T and Kelly D T, editors, *Atherosclerosis. Gene expression, cell interactions and oxidation*, pages 1–23. Oxford University Press, New York, USA, 2000.

P. Zunino. Multidimensional pharmacokinetic models applied to the design of drug-eluting stents. *Cardiovascular engineering: An International Journal*, 4(2):181–191, 2004.